Gas-Phase Inorganic Chemistry: Monovalent Derivatives of Calcium and Strontium

PETER F. BERNATH

The chemistry and spectroscopy of monovalent derivatives of calcium and strontium are described. Laser-driven chemical reactions of calcium and strontium vapors with a variety of small molecules have provided many new free radicals. In general, these species are analogous to the stable molecules obtained in traditional inorganic or organometallic chemistry, but some new families of molecules have been discovered.

THE INTERACTION OF METALS WITH ORGANIC MOLECULES IS one of the primary themes of modern chemistry. The activity in this area is driven by the fascinating variety of possible molecules and the lure of important applications. For example, the Ziegler-Natta polymerization of ethylene to make high-density polyethylene involves the interaction of ethylene with a Ti metal center (*1, 2*). Many biological molecules, such as hemoglobin, require the presence of a metal ion in order to function (*1*).

Almost all of the known metal-ligand chemistry occurs in solution and is therefore influenced by the presence of a solvent. In recent years the interaction of metals with organic and inorganic molecules in the gas phase has begun to be studied. Because the mass spectrometer is an exquisitely sensitive detector, most of this gas-phase work involves ions (*3*). The techniques used include traditional high-pressure mass spectrometry (*4*), flowing afterglows (*5*), ion beams (*6*), and Fourier transform ion cyclotron resonance (*7*). In this article the gas-phase chemistry and spectroscopy of a variety of new neutral species are reviewed.

In the past few years my research group and others have studied the molecules in Table 1 (*8–34*). These monovalent derivatives of Ca and Sr were made by laser-driven chemical reactions and detected by laser-induced fluorescence. Although some of these free radicals [MOH (*8–10*), $MOCH_3$ (*11*), MNH_2 (*8, 12*), and MNC (*13*), where M is Ca or Sr] were known before our work, we have systematically developed the gas-phase chemistry of Ca and Sr.

Background

Monovalent, free radical derivatives of the alkaline earth metals, such as CaOH, have a surprisingly long history. Although CaOH is very reactive and can only be isolated for extended periods of time in rare gas matrices (*35*), substantial concentrations occur in a variety of energetic environments.

In 1823 Herschel published his observations of the colors produced by alkaline earth metal salts in flames (*36*). Similar emission is seen, for example, in the red spectrum of fireworks made with Sr salts (*37*). By the mid-1950s it was clear that these colors were due to electronic transitions of the alkaline earth monohydroxide free radicals, such as CaOH and SrOH (*38, 39*). Since then there have been numerous additional flame investigations (*40, 41*) of these molecules because of the importance of flame absorption and emission measurements in analytical chemistry.

The alkaline earth hydroxides are also of interest in astronomy and atmospheric chemistry. Tsuji predicted that the alkaline earth monohydroxides should be abundant in the atmospheres of cool stars (*42*), and there has been a tentative detection of the electronic spectrum of CaOH in an M-type star (*43*). The surprisingly small dipole moment of CaOH (*44*) would make the microwave detection of CaOH relatively difficult in other astronomical sources, such as dark interstellar clouds. It has also been speculated that alkaline earth monohydroxides are formed in the earth's upper atmosphere from metals released either by man (*45*) or by ablation from meteors (*46*).

Other work on the alkaline earth hydroxides includes the measurement of dissociation energies and ionization potentials by mass spectrometry (*47*). Electron spin resonance (*48*) and infrared absorption spectra of matrix-isolated molecules (*35*) have been published. Ab initio calculations of the electronic structures are available (*49, 50*).

The key discovery, which led directly to the work reviewed here, was made by Harris and co-workers (*8–10*). They found that the alkaline earth hydroxides were easily made in a metal flow reactor called a Broida oven. The combination of a relatively cool molecular source (~500 K, much less than the traditional arcs or carbon furnaces) and single-frequency tunable dye laser excitation made detailed analysis of the spectra possible. Moreover, Harris and co-workers discovered a new family of isoelectronic derivatives, the alkaline earth monoamides, $CaNH_2$, $SrNH_2$, and $BaNH_2$ (*8, 12*), which pointed the way to the extensive chemistry reviewed here. The work of Harris and the work reviewed here were built on the

Table 1. Free radicals containing Ca and Sr, where M = Ca or Sr and R = H, CH_3, CH_2CH_3, and so forth.

Monohydroxides (*8–10, 14, 15*)	M–OH	Monohydrosulfides (*24*)	M–SH
Monoalkoxides (*11, 16, 17*)	M–O–R	Monoalkylamides (*8, 12, 25, 26, 32*)	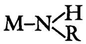 $M{-}N\begin{smallmatrix}H\\R\end{smallmatrix}$
Monocarboxylates (*18*)	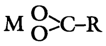 $M\begin{smallmatrix}O\\O\end{smallmatrix}C{-}R$	Monothiolates (*24*)	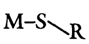 $M{-}S{-}R$
Monoformamidates (*19*)	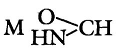 $M\begin{smallmatrix}O\\HN\end{smallmatrix}CH$	Monomethyls (*27*)	$M{-}CH_3$
		Monoacetylides (*28, 33*)	M–CCH
Monoisocyanates (*20, 21*)	M–NCO	Monocyclopentadienides (*29, 34*)	$M{-}C_5H_5$
Monoazides (*22*)	M–NNN	Monopyrrolates (*30*)	$M{-}C_4H_4N$
Monoisocyanides (*13, 23, 33*)	M–NC	Monoborohydrides (*31*)	$M{-}BH_4$

The author is in the Centre for Molecular Beams and Laser Chemistry, Department of Chemistry, University of Waterloo, Waterloo, Ontario, Canada N2L 3G1, and the Department of Chemistry, University of Arizona, Tucson, AZ 85721.

pioneering efforts of the late H. P. Broida.

During the course of work on alkaline earth derivatives, my research group found that laser excitation of the metal atom promotes the chemical reactivity of Ca, Sr, and Ba vapors. For example, the reaction (*20, 21*)

$$\mathrm{Ca^*(^3P_1) + HNCO \rightarrow CaNCO + H}$$

proceeds readily with Ca atoms excited to the $^3P_1$ state, whereas ground-state Ca ($^1S_0$) is nearly unreactive. Thus, one laser drives the chemical reaction while a second laser is used to detect the CaNCO product. This laser-induced chemical reactivity was vital in the preparation of most of the free radicals listed in Table 1. Our observations on the enhanced and sometimes selective reactivity of excited metal atoms are related to work by many other groups (*6, 51–53*).

Simple metal-containing free radicals such as CaOH are often called high-temperature molecules because an oven is used for metal vaporization or because the radicals are found in flames. In fact, the "high temperature" of a Broida oven is only slightly above room temperature because a room-temperature carrier gas such as Ar sweeps the metal vapor out of the vaporization region. Sometimes, however, even lower temperatures are desirable, for example, to resolve the rotational structure of a large molecule such as $\mathrm{CaOC(CH_3)_3}$. In this case a laser-vaporization source, coupled with supersonic expansion into vacuum and laser detection, is very convenient. The recent discovery of YNH by Simard *et al.* (*54*) and the work at Ohio State (*34, 55*) and Orsay (*32, 33*) on some of the alkaline earth derivatives of Table 1 illustrate the potential of this technique. Ellis, Robles, and Miller (*34*) have discovered $\mathrm{Cd(C_5H_5)}$ using this method.

Experimental Methods

The monovalent alkaline earth derivatives are produced in my laboratory in a Broida-type oven (*56*), a flow reactor that produces molecules by the reaction of a metal vapor with an appropriate oxidant (Fig. 1). The metal (Ca or Sr) is vaporized in a resistively heated alumina crucible and entrained in a flow of Ar gas. The oxidant is added at the top through an oxidant ring. The metal-oxidant reaction (for example, Ca + H_2O) often produces a low-pressure chemiluminescent flame above the oxidant ring (Fig. 1). Typical pressures are 3 torr of Ar gas, 1 mtorr of metal vapor, and 10 mtorr of oxidant. The resulting product molecule concentration is less than 1 mtorr, perhaps 10^{13} molecules per cm^3, under the most favorable circumstances.

The laser beams are usually introduced into the Broida oven through the top window (Fig. 2). Two dye lasers are used, one to drive the chemistry by providing excited metal atoms and the other to excite emission from the product molecules. The output of the first dye laser (DCM dye, Exciton, Dayton, Ohio) was tuned to the $^3P_1$-$^1S_0$ Ca atomic transition at 6573 Å or the corresponding Sr transition at 6892 Å. The second dye laser was operated with DCM dye (6200 to 7000 Å) or Pyridine 2 (Exciton, Dayton, Ohio) dye (6900 to 7900 Å). While the first laser was operated broadband (~1 cm^{-1} linewidth), the second laser was operated either broadband for survey work or in single longitudinal mode (~1 MHz bandwidth) for high-resolution work. Typical laser powers were 0.5 W. The two laser beams were spatially overlapped and focused into the Broida oven (Fig. 2).

The first laser beam was modulated by amplitude at ~1 kHz with an optical chopper, which modulates the concentration of excited Ca and Sr atoms. Because excited Ca and Sr atoms have a much higher reactivity, the concentration of product molecules was modulated at the same frequency. The modulated fluorescence excited by the second laser was detected by photomultiplier tube detectors and lock-in amplifiers. A monochromator or a set of optical filters was used to analyze the emission and control the optical bandwidth detected by the photomultiplier tubes.

Fig. 1. The baseplate for the Broida oven metal flow reactor. This baseplate is attached to the bottom of a vacuum chamber (Fig. 2). (a) Chemiluminescent flame; (b) oxidant injection ring; (c) tungsten wire heating basket; (d) Ar carrier gas inlet; (e) cooling water; (f) oxidant gas inlet; (g) electrical feeds for heating; (h) Ca or Sr metal; (i) alumina crucible; and (j) alumina heat shield.

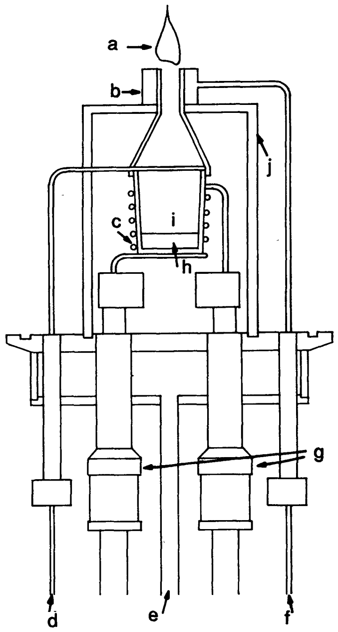

The high-resolution spectra recorded with a Broida oven are limited by the effects of Doppler broadening and collisional relaxation. For example, the Doppler full-width at half maximum of a rotational line is about 0.03 cm^{-1} for a molecule such as CaCCH. The technique of laser excitation spectroscopy with selective detection of fluorescence is necessary to sort out the complex rotational structure of a molecule such as $\mathrm{CaCH_3}$ (*27*). Collisional redistribution of the excited state population in the Broida oven thwarts this technique and prevents the rotational analysis of large molecules such as $\mathrm{Ca(C_5H_5)}$.

Gas-Phase Inorganic Chemistry

In 1983 we began to analyze some of the optical spectra of CaOH, SrOH, and BaOH. These molecules were made by the reaction of ground-state Ca, Sr, and Ba atoms with H_2O. In 1984 an attempt was made to make strontium monoacetylides or carbides (SrCCH or $\mathrm{SrC_2}$) by reaction of acetylene (HC≡CH) with Sr vapor. The laser excitation spectrum displayed in Fig. 3 was recorded. The sharp features could be assigned to the $\tilde{A}^2\Pi$-$\tilde{X}^2\Sigma^+$ electronic transition of SrOH and to the Sr $^3P_1$-$^1S_0$ atomic transition.

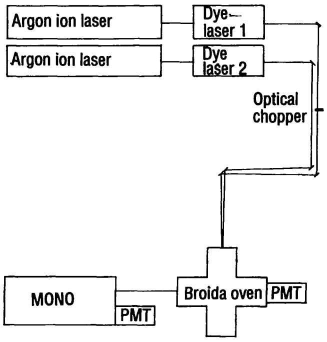

Fig. 2. Experimental block diagram. Two Ar ion lasers pump two dye lasers that are used to make and detect the free radicals in the Broida oven. The laser-induced fluorescence is monitored with photomultiplier tube (PMT) detectors mounted either directly on the oven or on the exit port of a monochromator (MONO).

The identity of the two broad features in Fig. 3 was more difficult to establish. After considerable spectroscopic and chemical detective work these new features were assigned to strontium monoisopropoxide [$SrOCH(CH_3)_2$]. This unusual free radical had formed from the gas-phase reaction of Sr with trace amounts of acetone (CH_3COCH_3) present in the acetylene. Welding-grade acetylene is dissolved in acetone to prevent explosive polymerization. The accidental overlap between the Sr atomic line and the Sr isopropoxide (Fig. 3) led to the discovery that excitation of the Sr ($^3P_1$-$^1S_0$) atomic transition led to the production of at least three orders of magnitude more strontium isopropoxide product than is produced without laser excitation.

At that time, the gas-phase reactivity of Sr and Ca vapors with acetone (discovered by serendipity) seemed remarkable. Acetone is a common chemical, not particularly noted for its reactivity. We reasoned that perhaps other common molecules would react with laser-excited Ca and Sr vapors. This has indeed proved to be the case, and a wide variety of monovalent derivatives of Ca and Sr are now known (Table 1). Eventually the SrCCH (*28*) molecule was made after removal of the acetone impurity from the acetylene gas.

Electronic Structure

One of the most appealing aspects of the spectroscopy of the monovalent alkaline earth derivatives is that a simple, one-electron, hydrogenic picture provides a reasonable picture of the electronic structure. This is not usually the case for the derivatives of the other elements of the periodic table. In fact, the major impediment to extending our work to the more chemically interesting transition elements is that the spectra will be difficult to interpret because of the presence of many states with large spin and orbital angular momenta.

One can best explain the electronic structure of the polyatomic monovalent alkaline earth derivatives (Fig. 4) by considering them to be ionic molecules like CaF, for example, Ca^+OH^-. The electronic structure of the isovalent alkaline earth monohalides is well known (*57–59*). CaOH is linear, rather than bent like H_2O or CaSH, because there is a partial positive charge on the proton of the OH^- group. The linear geometry maximizes the distance between the Ca^+ unit and the proton. As the ligand becomes less electronegative (for example, SH instead of OH), the degree of covalency in the metal-ligand bond increases, and the CaSH molecule is bent rather than linear.

The neutral Ca atom has an $[Ar]4s^2$ electronic configuration, and when Ca^+OH^- forms, one electron is transferred. The remaining $4s$ valence electron on Ca^+ is nonbonding and makes the $\tilde{X}^2\Sigma^+$ ground state of CaOH. The first and second excited states of Ca^+ result from promotion of the $4s$ electron to $3d$ and $4p$ states (Fig. 4). The $\tilde{A}^2\Pi$ and $\tilde{B}^2\Sigma^+$ states of CaOH originate from the $p\pi$ and $p\sigma$ orbitals correlating with the $4p$ Ca^+ orbital mixed with the $d\pi$ and $d\sigma$ orbitals correlating with the $3d$ Ca^+ orbital. The $\tilde{B}^2\Sigma^+$ and $\tilde{A}^2\Pi$ states are $p\sigma$-$d\sigma$ and $p\pi$-$d\pi$ orbital mixtures polarized to keep the unpaired electron as far from the OH^- group as possible.

In a bent molecule such as CaSH, the degeneracy of the two components of the "$\tilde{A}^2\Pi$" state is lifted, and in-plane $\tilde{A}^2A'$ and out-of-plane $\tilde{B}^2A''$ states result. The $\tilde{B}^2\Sigma^+$ state of CaOH must then correlate with the $\tilde{C}^2A'$ of CaSH (Fig. 4). In simple terms the $\tilde{A}$-$\tilde{X}$, $\tilde{B}$-$\tilde{X}$, and $\tilde{C}$-$\tilde{X}$ electronic transitions of CaSH could be described as the three components of the p (p_x, p_y, p_z) $\leftarrow$ s resonance transition of Ca^+ perturbed by the presence of an SH^- ligand.

These qualitative descriptions of electronic structure can be made quantitative by the tools of modern quantum chemistry. Ortiz has calculated the electronic structure of CaOH (*50*) and CaSH (*60*) using ab initio electron propagator techniques. His calculations (*50, 60–62*) agree well with our observations, and they seem to have captured the simple one-electron character of the electronic transitions.

Isoelectronic Analogies

The study of gas-phase chemistry of Ca and Sr is aided by the usual isovalent and isoelectronic analogies based on the periodic table of elements. Consider the monovalent, isoelectronic family of molecules CaF, CaOH, $CaNH_2$, and $CaCH_3$. The periodic table of elements suggested to us that $CaBH_4$ was the last potential member of this isoelectronic series.

Ground-state Ca atoms were found to react with diborane, B_2H_6, to make $CaBH_4$ (*31*). The low-resolution spectra of the $\tilde{B}^2E$-$\tilde{A}^2A_1$ and $\tilde{B}^2A_1$-$\tilde{X}^2A_1$ electronic transitions of $CaBH_4$ are consistent (Table 2) with a tridentate, bridging structure of C_{3v} symmetry. The high-resolution analysis of $CaBH_4$ has not been completed, so the

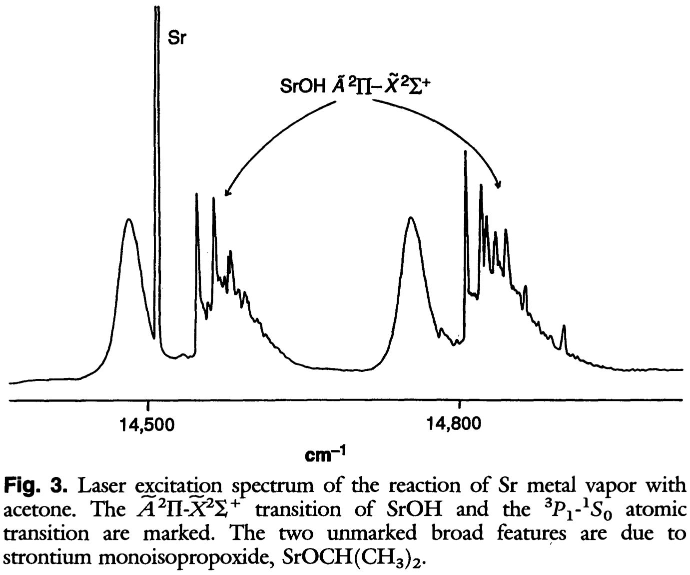

Fig. 3. Laser excitation spectrum of the reaction of Sr metal vapor with acetone. The $\tilde{A}^2\Pi$-$\tilde{X}^2\Sigma^+$ transition of SrOH and the $^3P_1$-$^1S_0$ atomic transition are marked. The two unmarked broad features are due to strontium monoisopropoxide, $SrOCH(CH_3)_2$.

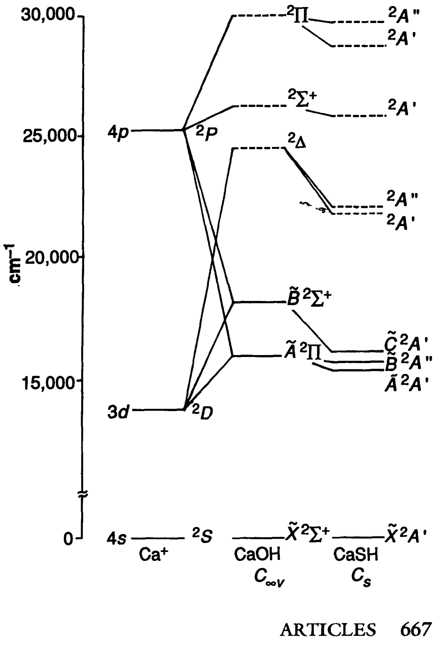

Fig. 4. Energy correlation diagram for Ca^+, CaOH, and CaSH. The solid horizontal lines are known energy levels, whereas the dashed lines are the ab initio predictions of Ortiz (*50, 60*).

Table 2. Observed spin-orbit splittings (in cm^{-1}) for the $\tilde{A}^2\Pi$ or $\tilde{A}^2E$ states of some free radicals containing alkaline earth metals, ML, where M = Ca or Sr, and L is a ligand.

Molecule	CaL	SrL
MOH (*8–10, 14, 15*)	67	264
$MOCH_3$ (*11, 16, 17*)	65	268
MCCH (*28, 33*)	70	275
MN_3 (*22*)	76	296
MNCO (*20, 21*)	68	293
MCH_3 (*27*)	73	309
MBH_4 (*31*)	59	200
MC_5H_5 (*29*)	57	255
MC_4H_4N (*30*)	76	300

C_{3v} structure is not proven, although it is consistent with the ab initio calculations (*61*).

Isocyanates and Azides

The NCO^- and NNN^- anions are often called pseudohalides (*63*) because they have a chemistry similar to that of F^-, Cl^-, Br^-, and I^-. The CaNCO and SrNCO molecules were made by treating the excited Ca or Sr atoms with HNCO (*20, 21*). The detection of the $\tilde{A}^2\Pi$-$\tilde{X}^2\Sigma^+$ and $\tilde{B}^2\Sigma^+$-$\tilde{X}^2\Sigma^+$ electronic transitions at low resolution suggested linear structures, but there is the possibility of linkage isomers (*20*). Is the structure CaNCO (calcium monoisocyanate) or CaOCN (calcium monocyanate)? In our initial paper we incorrectly guessed CaOCN (*20*).

To determine the structure of the MNCO molecules, we made CaN_3 and SrN_3. Ca and Sr vapors react spontaneously with HN_3 to give the desired monoazide derivatives (*22*), and again, linear structures were found.

Finally, a rotational analysis of the $\tilde{A}^2\Pi$-$\tilde{X}^2\Sigma^+$ transition was completed for SrN_3 (*22*) and SrNCO (*21*). For the ground $\tilde{X}^2\Sigma^+$ states, the rotational constants, *B*, were found to be 0.0448635(13) cm^{-1} for SrN_3 and 0.0425807(51) cm^{-1} for SrNCO (the numbers in parentheses are the errors in the last digits). If reasonable ligand geometries are assumed, the metal ligand bond lengths can be calculated from the moments of inertia to be 2.26 Å in both cases. This is strong evidence for the SrNCO structure because the Sr–O bond length was found to be 2.11 Å (much different) in $SrOCH_3$ (*17*) and SrOH (*9*). In addition, the Sr–N bond length in $SrNH_2$ was also found to be 2.25 Å (*26*), again supporting the idea of a characteristic Sr–N bond length.

SrN_3, CaN_3, SrNCO, and CaNCO are prototypical molecules. Gas-phase ionic azides and isocyanates had not been spectroscopically characterized previously. When other ionic azide and isocyanate molecules such as KN_3 or NaNCO are discovered, geometric structures similar to the alkaline earth examples are anticipated.

Cyclopentadienides and Pyrrolates

The cyclopentadienyl (Cp = C_5H_5) ligand is one of the most useful and fascinating ligands in inorganic chemistry (*1*). The most celebrated molecule containing the Cp ligand is the sandwich complex ferrocene, $Fe(Cp)_2$. We synthesized the "open-faced sandwich" complexes CaCp and SrCp (*29*) by the interaction of excited metal atoms with cyclopentadiene:

$$Ca^* + C_5H_6 \rightarrow Ca(C_5H_5) + H$$

The observation of the $\tilde{A}^2E_1$-$\tilde{X}^2A_1$ and $\tilde{B}^2A_1$-$\tilde{X}^2A_1$ electronic transitions suggests that CaCp and SrCp (Fig. 5A) have pentagonal symmetry (C_{5v}). Our observations have recently been confirmed by the jet-cooled spectrum of CaCp recorded by Ellis, Robles, and Miller (*34*). The electronic structure is similar to that of CaOH (Fig. 4), but the names of the states have to be changed ($\tilde{A}^2\Pi$ to $\tilde{A}^2E_1$ and $\tilde{B}^2\Sigma^+$ to $\tilde{B}^2A_1$) because of the lower symmetry of the cyclopentadienide complexes.

The $\tilde{A}^2E_1$ electronic state shows no sign of a Jahn-Teller distortion (*1*). The spin-orbit and Jahn-Teller effects compete, and, in this case, the $\tilde{A}^2E_1$ state splits into two spin-orbit components, $\tilde{A}^2E_{1(1/2)}$ and $\tilde{A}^2E_{1(3/2)}$. The splitting between the two spin components is 55 cm^{-1} for CaCp and 67 cm^{-1} for CaOH. The presence of five off-axis carbons and hydrogens hardly quenches the spin-orbit coupling, because the $\tilde{A}^2E_1$ state has the unpaired electron polarized away from the Cp ring so that the unpaired electron is separated from the ring by the Ca^{2+} metal atom. The ab initio calculations of Ortiz (*62*) support this picture of the unpaired electron distributions in CaCp. The unpaired electron is, therefore, only slightly affected by the nature of the ligand.

Although the cyclopentadienyl ligand is very common in organometallic chemistry, isoelectronic pyrrolyl derivatives are rare (*1*). For example, azaferrocene $(C_4H_4N)Fe(C_5H_5)$ is known (*64*), but diazaferrocene $Fe(C_4H_4N)_2$ has yet to be isolated. Pyrrole is isoelectronic with cyclopentadiene, with the CH_2 group of C_5H_6 replaced by the NH group in C_4H_5N. Loss of the proton from the N atom in C_4H_5N makes the pyrrolate anion $C_4H_4N^-$ isoelectronic with $C_5H_5^-$.

In the gas phase, however, the reaction of laser-excited Ca vapor with pyrrole makes the monopyrrolate derivative,

$$Ca^* + C_4H_5N \rightarrow Ca(C_4H_4N) + H$$

The "$\tilde{A}^2E$"-$\tilde{X}^2A_1$ and "$\tilde{B}^2A_1$"-$\tilde{X}^2A_1$ electronic transitions were observed, suggesting ring bonding for the pyrrolate derivatives. The pyrrolate ligand ($C_4H_4N^-$) could bond through the N atom to make η^1-monopyrrolates of C_{2v} symmetry (like $CaNH_2$), or the pyrrolate ligand could ring bond, making η^5-monopyrrolates (Fig. 5B) of "pseudo-C_{5v}" symmetry. The electronic spectrum of $Ca(C_4H_4N)$ resembles that of $Sr(C_5H_5)$ rather than those of the metal monoamides, $CaNH_2$ and $SrNH_2$. While this is hardly conclusive evidence, it suggests that as far as the electronic structure (Table 2) is concerned, the pyrrolate derivatives behave as if they had nearly pentagonal (C_{5v}) symmetry and are ring bonding. These

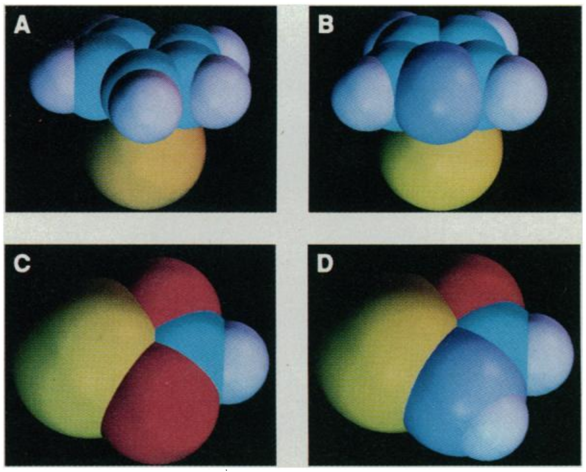

Fig. 5. (**A**), Calcium monocyclopentadienide free radical, $Ca(C_5H_5)$; (**B**), calcium monopyrrolate free radical, $Ca(C_4H_4N)$; (**C**), calcium monoformate free radical, Ca(HCOO); (**D**), calcium monoformamidate free radical, Ca(HCONH).

arguments are supported by recent work by Miller and co-workers on pyrrolyl derivatives of group IIB atoms (*65*).

Formates and Formamidates

How is the gas-phase inorganic chemistry of Ca and Sr different from the known chemistry of the elements? Monographs on inorganic chemistry (*1, 66*) provide us with guidance in our search for new molecules. However, the gas-phase chemistry of alkaline earth–containing free radicals might be expected to be different than the conventional chemistry of stable substances. The monoformamidate derivatives of Ca and Sr, which we discovered, are an example of molecules for which there are no corresponding analogues in inorganic chemistry.

Formamide, $HCONH_2$, is isoelectronic with formic acid, HCOOH, and removal of a proton gives the formamidate anion $HCONH^-$ (compare with $HCOO^-$). A few research groups have studied the substitution of formate ligands by amidato ligands in, for example, $Rh_2(ONHCCF_3)_4$ (*67*), but there are no reports of molecules with the formamidate ligand.

In the gas phase the reaction

$$\mathrm{Ca}^* + \mathrm{HCONH_2} \rightarrow \mathrm{Ca(HCONH)} + \mathrm{H}$$

occurs readily, as does the corresponding reaction with HCOOH. The calcium monoformate molecule has a bidentate structure (Fig. 5C) and three electronic transitions $\tilde{A}\,^2A_1$-$\tilde{X}\,^2A_1$, $\tilde{B}\,^2B_2$-$\tilde{X}\,^2A_1$, and

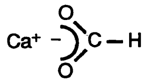

$\tilde{C}\,^2B_1$-$\tilde{X}\,^2A_1$ (*18*), like CaSH. The $\tilde{B}\,^2\Sigma^+$ state of CaOH becomes the $\tilde{A}\,^2A_1$ state of Ca(HCOO), and the $\tilde{A}\,^2\Pi$ state of CaOH seems to correlate with the $\tilde{B}\,^2B_2$ and $\tilde{C}\,^2B_1$ states (*18*). Because the high-resolution spectrum of the Ca(HCOO) molecule has not been recorded, the ordering of the excited states of B_2, B_1, and A_1 symmetry is not established with certainty. The spectrum of Ca(HCONH) is similar to that of Ca(HCOO), with three electronic transitions, $\tilde{A}\,^2A'$-$\tilde{X}\,^2A'$, $\tilde{B}\,^2A'$-$\tilde{X}\,^2A'$, and $\tilde{C}\,^2A''$-$\tilde{A}\,^2A'$ (compare with CaSH, Fig. 4), observed. Presumably the Ca(HCONH) molecule has a bidentate structure (Fig. 5D) by analogy with Ca(HCOO).

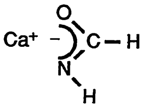

Surprisingly, Ca reacts with formic acid (but not formamide) without laser excitation of the metal atom. Studies of the reactions of alkaline earth atoms with water in Ar matrices (*35*) suggest a possible mechanism. In an Ar matrix at 10 K the deposition of Ca and H_2O first produce a $Ca(OH_2)$ complex (*35*). Upon photolysis, the metal atom inserts to form the H–Ca–OH molecule, and on ultraviolet irradiation, the H–Ca–OH molecule dissociates to form CaOH (*35*).

The reaction of ground-state Ca atoms with formic acid might, therefore, proceed by the following mechanism:

$$\mathrm{Ca} + \mathrm{HCOOH} \xrightarrow{\mathrm{Ar}} \mathrm{HC(O)O{-}Ca{-}H}$$

$$\mathrm{HC(O)O{-}Ca{-}H} + \mathrm{Ca} \rightarrow \mathrm{CaH} + \mathrm{Ca(HCOO)}$$

$$\mathrm{CaH} + \mathrm{HCOOH} \rightarrow \mathrm{Ca(HCOO)} + \mathrm{H_2}$$

This mechanism is supported by the observation of CaH in the oven and by the increased production of Ca(HCOO) with increasing Ar carrier gas pressure (*18*). The study of both the chemistry and spectroscopy of Ca(HCOO) and Ca(HCONH) are at a very early stage, and more measurements are necessary.

Conclusion

We have discovered an extensive gas-phase chemistry of monovalent derivatives of Ca and Sr. Laser-driven chemical reactions of Ca and Sr vapors with a variety of small inorganic and organic molecules have provided many new free radicals. On the whole, the structures of these free radicals parallel the stable molecules obtained in traditional inorganic and organometallic chemistry. However, some new families of molecules, such as the metal monoformamidates Ca(HCONH), were discovered. Our methods have general utility for the synthesis and characterization of inorganic free radicals.

REFERENCES AND NOTES

1. F. A. Cotton and G. Wilkinson, *Advanced Inorganic Chemistry* (Wiley, New York, ed. 5, 1988).
2. R. H. Grubbs and W. Tumas, *Science* **243**, 907 (1989).
3. For example, *Gas Phase Inorganic Chemistry*, D. H. Russell, Ed. (Plenum, New York, 1989).
4. P. Kebarle, *Annu. Rev. Phys. Chem.* **28**, 445 (1977).
5. D. Smith and N. Adams, in *Gas Phase Ion Chemistry*, M. T. Bowers, Ed. (Academic Press, New York, 1979), vol. 1, pp. 1–44; see also vols. 2 and 3 of this series.
6. P. B. Armentrout, *Science* **251**, 175 (1991); *Annu. Rev. Phys. Chem.* **41**, 313 (1990).
7. For example, M. V. Buchanan, Ed., *Fourier Transform Mass Spectrometry*, vol. 359 of the *ACS Symposium Series* (American Chemical Society, Washington, DC, 1987).
8. R. F. Wormsbecher, M. Trkula, C. Martner, R. E. Penn, D. O. Harris, *J. Mol. Spectrosc.* **97**, 29 (1983).
9. J. Nakagawa, R. F. Wormsbecher, D. O. Harris, *ibid.*, p. 37.
10. R. C. Hilborn, Q. Zhu, D. O. Harris, *ibid.*, p. 73.
11. R. F. Wormsbecher and R. D. Suenram, *ibid.* **95**, 391 (1982).
12. R. F. Wormsbecher, R. E. Penn, D. O. Harris, *ibid.* **97**, 65 (1983).
13. L. Pasternack and P. J. Dagdigian, *J. Chem. Phys.* **65**, 1320 (1976); N. Furio and P. J. Dagdigian, *Chem. Phys. Lett.* **115**, 358 (1985).
14. P. Bernath and S. Kinsey-Nielsen, *Chem. Phys. Lett.* **105**, 663 (1984); P. F. Bernath and C. R. Brazier, *Astrophys. J.* **288**, 373 (1985); R. A. Hailey, C. N. Jarman, W. T. M. L. Fernando, P. F. Bernath, *J. Mol. Spectrosc.* **147**, 40 (1991).
15. C. R. Brazier and P. F. Bernath, *J. Mol. Spectrosc.* **114**, 163 (1985).
16. ———, S. Kinsey-Nielsen, L. C. Ellingboe, *J. Am. Chem. Soc.* **108**, 2126 (1986).
17. L. C. O'Brien, C. R. Brazier, P. F. Bernath, *J. Mol. Spectrosc.* **130**, 33 (1988).
18. L. C. O'Brien, C. R. Brazier, S. Kinsey-Nielsen, P. F. Bernath, *J. Phys. Chem.* **94**, 3543 (1990).
19. A. M. R. P. Bopegedera, W. T. M. L. Fernando, P. F. Bernath, *ibid.*, p. 3547.
20. L. C. Ellingboe, A. M. R. P. Bopegedera, C. R. Brazier, P. F. Bernath, *Chem. Phys. Lett.* **126**, 285 (1986).
21. L. C. O'Brien and P. F. Bernath, *J. Chem. Phys.* **88**, 2117 (1988).
22. C. R. Brazier and P. F. Bernath, *ibid.*, p. 2112.
23. M. Douay and P. F. Bernath, *Chem. Phys. Lett.* **174**, 230 (1990).
24. W. T. M. L. Fernando, R. S. Ram, L. C. O'Brien, P. F. Bernath, *J. Phys. Chem.* **95**, 2665 (1991).
25. A. M. R. P. Bopegedera, C. R. Brazier, P. F. Bernath, *ibid.* **91**, 2779 (1987).
26. C. R. Brazier and P. F. Bernath, unpublished results.
27. ———, *J. Chem. Phys.* **86**, 5918 (1987); *ibid.* **91**, 4548 (1989).
28. A. M. R. P. Bopegedera, C. R. Brazier, P. F. Bernath, *Chem. Phys. Lett.* **136**, 97 (1987); *J. Mol. Spectrosc.* **129**, 268 (1988).
29. L. C. O'Brien and P. F. Bernath, *J. Am. Chem. Soc.* **108**, 5017 (1986).
30. A. M. R. P. Bopegedera, W. T. M. L. Fernando, P. F. Bernath, *J. Phys. Chem.* **94**, 4476 (1990).
31. F. S. Pianalto *et al.*, *J. Am. Chem. Soc.* **112**, 7900 (1990).
32. C. J. Whitham and Ch. Jungen, *J. Chem. Phys.* **93**, 1001 (1990).
33. C. J. Whitham, B. Soep, J.-P. Visticot, A. Keller, *ibid.*, p. 991.
34. A. M. Ellis, E. S. J. Robles, T. A. Miller, *ibid.* **94**, 1752 (1991).
35. J. W. Kauffman, R. H. Hauge, J. L. Margrave, *High Temp. Sci.* **18**, 97 (1984).
36. J. F. W. Herschel, *Trans. R. Soc. Edinburgh* **9**, 445 (1823).
37. R. F. Barrow and E. F. Caldin, *Proc. Phys. Soc. London Sect. B* **62**, 32 (1949).
38. C. G. James and T. M. Sugden, *Nature* **175**, 333 (1955).
39. M. Charton and A. G. Gaydon, *Proc. Phys. Soc. London Sect. A* **69**, 520 (1956); A. G. Gaydon, *Proc. R. Soc. London Ser. A* **231**, 437 (1955).
40. For example, P. A. Bonczyk, *Combust. Flame* **59**, 143 (1988); M. B. Blackburn, J. M. Mermet, J. D. Winefordner, *Spectrochim. Acta Part A* **34**, 847 (1978).

41. C. Th. J. Alkemade, Tj. Hollander, W. Snelleman, P. J. Th. Zeegers, *Metal Vapours in Flames* (Pergamon, Oxford, 1982).
42. T. Tsuji, *Astron. Astrophys.* **23**, 411 (1973).
43. P. Pesch, *Astrophys. J.* **174**, L155 (1974).
44. C. W. Bauschlicher, Jr., S. R. Langhoff, T. C. Steimle, J. E. Shirley, *J. Chem. Phys.* **93**, 4179 (1990).
45. S. Drapatz, L. Haser, K. W. Michel, *Z. Naturforsch. Teil A* **29**, 411 (1974).
46. E. Murad, W. Swider, S. W. Benson, *Nature* **289**, 273 (1981); S. C. Lin and G. C. Reid, *Geophys. Res. Lett.* **6**, 283 (1979).
47. E. Murad, *J. Chem. Phys.* **75**, 4080 (1981).
48. J. M. Brom, Jr., and W. Weltner, Jr., *ibid.* **77**, 2057 (1982); *ibid.* **78**, 6611 (1983).
49. C. W. Bauschlicher, Jr., S. R. Langhoff, H. Partridge, *ibid.* **84**, 901 (1986).
50. J. V. Ortiz, *ibid.* **92**, 6728 (1990).
51. M. Menzinger, *Adv. Chem. Phys.* **42**, 1 (1980).
52. W. H. Breckenridge and H. Umemoto, *ibid.* **50**, 325 (1982).
53. P. J. Dagdigian and M. L. Campbell, *Chem. Rev.* **87**, 1 (1987).
54. B. Simard, W. J. Balfour, M. Vasseur, P. A. Hackett, *J. Chem. Phys.* **93**, 4481 (1990).
55. E. S. J. Robles, A. M. Ellis, T. A. Miller, *Chem. Phys. Lett.* **178**, 185 (1991).
56. J. B. West, R. S. Bradford, J. D. Eversole, C. R. Jones, *Rev. Sci. Instrum.* **46**, 164 (1975).
57. P. F. Bernath, B. Pinchemel, R. W. Field, *J. Chem. Phys.* **74**, 5508 (1981).
58. S. F. Rice, H. Martin, R. W. Field, *ibid.* **82**, 5073 (1985).
59. T. Törring, W. E. Ernst, J. Kändler, *ibid.* **90**, 4927 (1989).
60. J. V. Ortiz, *Chem. Phys. Lett.* **169**, 116 (1990).
61. ———, *J. Am. Chem. Soc.* **113**, 1102 (1991).
62. ———, *ibid.*, p. 3593.
63. A. M. Golub, H. Kohler, V. V. Skopenko, *Chemistry of the Pseudohalides* (Elsevier, Amsterdam, 1986).
64. K. K. Joshi, P. L. Paulson, A. R. Qazi, W. H. Stubbs, *J. Organomet. Chem.* **1**, 471 (1964).
65. E. S. J. Robles, A. M. Ellis, T. A. Miller, paper RB4, presented at the Forty-Sixth International Symposium on Molecular Spectroscopy, Columbus, Ohio, 17 to 21 June 1991.
66. N. N. Greenwood and A. Earnshaw, *Chemistry of the Elements* (Pergamon, Oxford, 1984).
67. A. M. Denis, J. D. Korp, I. Bernal, R. A. Howard, J. L. Bear, *Inorg. Chem.* **22**, 1522 (1983).
68. I thank my students and collaborators, C. Brazier, A. M. R. P. Bopegedera, L. O'Brien, W. T. M. L. Fernando, S. Kinsey-Nielsen, S. Pianalto, R. Hailey, M. Douay, R. Ram, and C. Jarman, for their invaluable contributions to the work summarized here. This work was supported by the NSF, Petroleum Research Fund, Office of Naval Research, Research Corporation, Natural Science and Engineering Research Council of Canada, and the Astronautics Laboratory, Edwards Air Force Base. I acknowledge support as an Alfred P. Sloan Fellow and a Camille and Henry Dreyfus Teacher-Scholar. I thank K. Walker and A. Tang for assistance with the figures.

Stress Fields of the Overriding Plate at Convergent Margins and Beneath Active Volcanic Arcs

K. DENISE APPERSON

Tectonic stress fields in the overriding plate at convergent plate margins are complex and vary on local to regional scales. Volcanic arcs are a common element of overriding plates. Stress fields in the volcanic arc region are related to deformation generated by subduction and to magma generation and ascent processes. Analysis of moment tensors of shallow and intermediate depth earthquakes in volcanic arcs indicates that the seismic strain field in the arc region of many convergent margins is subhorizontal extension oriented nearly perpendicular to the arc. A process capable of generating such a globally consistent strain field is induced asthenospheric corner flow below the arc region.

CONVERGENT PLATE MARGINS PRODUCE THE WIDEST VARIATION in deformation styles of any tectonic environment. Principal tectonic features at convergent margins include the subducting plate and associated sediments, the interplate shear zone, and the overriding plate. The overriding plate may possess a forearc with a large deforming accretionary wedge (*1*), forearc basins and highs, a strong backstop beneath the forearc (*2*), a volcanic arc, and a backarc (*3*) (Fig. 1). Tectonic stress fields within the heterogenous convergent margin system are complicated as a result of local to regional variations in material properties, geometry of the plate boundary, and plate motions. Knowledge of regional stress fields is important for understanding how subduction and collision affect deformation of the overriding plate. In particular, characterization of stress fields in the volcanic arc region provides a link between forearc and backarc deformation and can help us understand magma generation and ascent processes.

A volcanic arc is a primary product of plate subduction and is a feature common to all margins where convergence is faster than a few centimeters per year and the dip of the subducting plate is not horizontal at depths of about 100 km. One of the most notable features of volcani arcs is their location, on average, 125 km above the Wadati-Benioff zone c of seismicity in the subducting plate (*4*, *5*). The spacing of volcanic centers varies considerably from arc to arc and along strike of a single arc, although through millions of years of activity many volcanic arcs exhibit a relatively regular and surprisingly narrow width of about 50 km (*4*).

Earthquakes beneath active volcanic arcs can occur in arc crust and lithosphere, possibly in the underlying asthenospheric wedge, and in the upper parts of the Wadati-Benioff zone (at depths around 100 to 200 km). In this article, I use strain information contained in summed earthquake moment tensors to characterize the seismic strain field of the volcanic arc region of overriding plates at active convergent margins. If we assume that the seismic strain fields are simply related to tectonic stress fields, we can examine the effects that subduction and magma generation processes have upon overriding plate deformation. As a context for interpretation of the data, I first review the general nature and controls of stresses in the overriding plate.

Tectonic Stress Fields and Deformation of Overriding Plates

In the 1970s, the conventional view was that subhorizontal compressive tectonic stresses were transmitted throughout the over-

---

The author is in the Department of Geological Sciences, University of Texas at Austin, Austin, TX 78713.